A kinetic approach to the mechanism of formation of mesoporous silica nanoparticles

Ricardo Alvarado Meza,[1] Tom Santori[1] and Xavier Cattoën[1,*]

[1]*Univ. Grenoble Alpes, CNRS, Grenoble INP, Institut Néel, 38000 Grenoble, France;*
xavier.cattoen@neel.cnrs.fr

ORCID 0000-0003-1072-0573 (X.C.)

Graphical Abstract

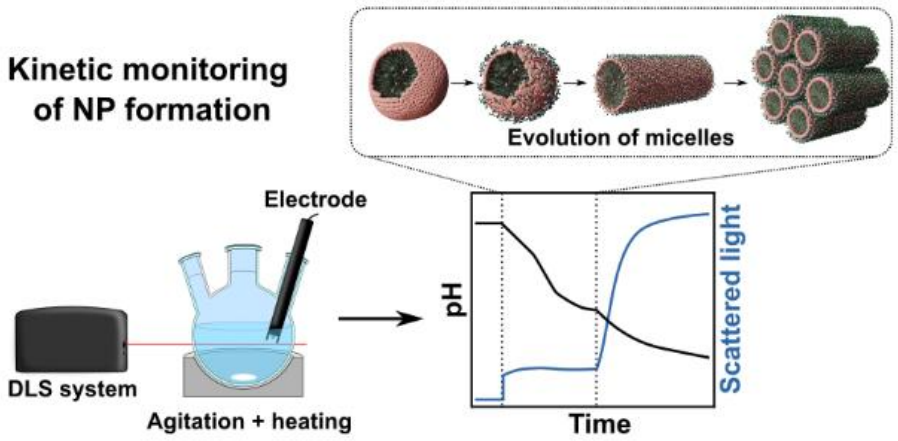

The synthesis of mesoporous silica nanoparticles was investigated by pH monitoring, which gives valuable complementary information to the currently accepted mechanism.

Keywords: kinetic studies; mechanism; Mesoporous Silica Nanoparticles; hydrolysis; condensation.

Abstract. The synthesis of mesoporous silica nanoparticles (MSNs), widely investigated for application in nanomedicine, depends on many experimental factors and lacks of reproducibility. Furthermore, its mechanism is not fully understood, in particular for the chemistry of the hydrolysis and condensation of tetraethoxysilane (TEOS). We coupled simple pH measurements with light diffusion monitoring directly within the reaction vessel in order to understand the early stages of the synthesis until the formation of nanoparticles. We found out that two regimes of hydrolysis can be detected before the nanoparticles are formed. At the turning point, only 28% of the TEOS molecules are singly hydrolyzed and the condensation reaction only starts after the aggregation of the silicate-surfactant micelles. Experimental factors such as stirring strength or carbonatation of sodium hydroxide exert a strong influence on the kinetics of MSNs formation and on their size, and must be carefully controlled for reproducibility. Based on all our experimental evidence and on previous literature reports, the formation mechanism was completed in order to highlight the importance of the interplay between chemical and physico-chemical processes in such a complex system.

Highlights:

- pH monitoring coupled with light scattering measurements enable understanding the early stages of the synthesis of MSNs promoted by sodium hydroxide.
- The nucleation of the nanoparticles, determining step to control their size, occurs within a minute after the initial TEOS addition under basic conditions.
- Two regimes of hydrolysis are observed initially, while the condensation reaction only starts after the nucleation of NPs.
- Experimental factors such as stirring strength or carbonatation of sodium hydroxide must be carefully controlled for reproducibility.

Acknowledgements

Sabine Douillet and Dr Jérôme Kieffer (ESRF) are gratefully acknowledged for their help.

Introduction

Mesoporous silica nanoparticles (MSNs) are being widely investigated for applications in nanomedicine, owing to their elevated porosity, rigidity, biocompatibility and ease for further surface modifications [1]. Their synthesis is usually performed by sol-gel reactions from tetraethoxysilane (TEOS) in the presence of cetyltrimethylammonium bromide (CTAB, CTA^+, Br^-) as structure-directing agent. Though multiple preparation methods have been reported to date in order to control their size and texture,[1–6] two main systems are employed: (i) ammonia-based recipes, where ammonia acts both as basic and nucleophilic catalyst; (ii) sodium hydroxide-based recipes, where the hydroxide ions mainly act as basic catalysts for the hydrolysis and condensation reactions. In the latter case, the usual protocol consists in adding TEOS to a basic solution of CTAB at 80 °C.[7] Multiple parameters have been varied to control the size and dispersity of the MSNs, and the use of statistical design of experiments helped to find optimal conditions.[8–10] In particular, the sodium hydroxide initial concentration has been found to play a key role in controlling the size, a higher initial pH leading to larger MSNs.[8–13] Accordingly, the determining factor governing the MSNs' size is indeed the ionic strength at which silicate-micelles composites aggregate, a larger ionic strength leading to larger particles as a result of increased charge screening between individual linear CTA^+-silicate micelles, enabling larger assemblies.[12] This was indeed shown by systematically varying the ionic strength using sodium chloride with identical initial pH.

pH plays a crucial rule in silica syntheses, affecting both the kinetics of hydrolysis and condensation. The hydrolysis reaction, enabled both by acids and bases is the slowest under neutral conditions,[14] whereas the condensation reactions are the slowest near the isoelectric point of silica at pH~2. Under basic conditions, the hydrolysis rate increases linearly with the hydroxide concentration according to equation (1). This allows monitoring the hydrolysis reaction kinetics by pH measurements.[15] In turn, the condensation reactions (equations (2) and (3)) release hydroxide anions, resulting in a pH increase. The balance between hydrolysis and condensation reactions can thus be easily monitored during the reaction. However, this simple technique has never been applied to understand the initial stages of the MSNs synthesis.[15, 16]

Hydrolysis: $\equiv Si\text{—}OEt + OH^- \rightarrow \equiv Si\text{—}OH + EtO^- \rightarrow \equiv Si\text{—}O^- + EtOH$ (1)

Condensation: $\equiv Si\text{—}O^- + \equiv Si\text{—}OEt + H_2O \rightarrow \equiv Si\text{—}O\text{—}Si\equiv + EtOH + HO^-$ (2)

$\equiv Si\text{—}O^- + \equiv Si\text{—}OH \rightarrow \equiv Si\text{—}O\text{—}Si\equiv + HO^-$ (3)

Besides, TEM at various stages has been used to follow the initial stages of MSNs formation in the case of a synthesis using the dilution of a concentrated mixture right after nucleation. Under those conditions, small (*ca* 5 nm) ellipsoidal clusters were first observed, which then aggregated to form larger objects (*ca* 50 nm) which internally reorganized to yield surfactant-silicate nanocomposites with an internal 2D symmetry.[17] Small angle neutron scattering was used [18] for systems employing tetramethoxysilane as precursor and triethanolamine as basic and nucleophilic catalyst, but which also forms atrane complexes thus involving a substantially different mechanism compared to the simple MSN synthesis.[19] Interestingly, this study revealed that the mechanism likely begins with the adsorption of hydrolyzed or slightly condensed silanolates at the surface of positively charged CTA^+ micelles, followed by the aggregation of those micelles to form nanoobjects as the charge per micelle decreases. These objects likely further aggregate to form larger nanoparticles. SAXS studies were also employed which allowed to understand the evolution of the micellar phase during the process.[20] This study gave insights into the evolution of the CTA^+ micelles during the synthesis, but again for conditions (pH or temperature) significantly different from those usually applied for the synthesis of MSNs and with an elevated concentration of CTAB (82 mM) likely necessary to get sufficient scattering signal. Interestingly, this study revealed that the addition of TEOS would first lead to a swelling of the initially ellipsoidal CTA^+ micelles, with the hydrolysis of TEOS occurring at their

surface. During the reaction, the micelles would then shrink as the TEOS is consumed and the obtained anionic silicates move towards the aqueous phase.

So far, the mechanistic investigations rely either on the initial and final state of the system varying synthesis parameters such as base concentration and salt addition,[8, 11–13] and on SAXS or SANS in a flow cell and under conditions that slow down the processes.[18, 20, 21] In the present study, we decided to monitor the formation of MSNs within the reaction vessel, trying not to disturb the reacting system. In particular we decided to use pH monitoring and light scattering to investigate the early stages of this sol-gel reaction. Together with the data found in the literature, the obtained results enable a deeper understanding on the interplay between physical processes and chemical reactions in these syntheses that lack of reproducibility, and for which scale up is still a significant challenge [10, 11].

Experimental section

Hexadecyltrimethylammonium bromide (CTAB, H5882), tetraethyl orthosilicate (TEOS), and all other reagents were purchased from Sigma-Aldrich. Fresh sodium hydroxide solutions were prepared every day (2.0 M, NaOH). Gradient HPLC grade water (Fisher) was used in all syntheses. The reaction temperature was controlled within the reaction medium and was set to 80 °C ± 1 °C unless otherwise stated.

The pH was monitored using a SevenEasy pHmeter from Mettler Toledo, with a pH inlab expert electrode working from 0 to 95 °C. pH values were transferred every second to a computer for further treatment. Scattering was measured using a VascoKin DLS equipment (Cordouan). The probe, which collects light backscattered at 173°, was located at a distance such that the focal point of the laser lied <1 mm from the wall of the reaction vessel. Field effect scanning electron microscopy (SEM) images were obtained on a Zeiss Gemini ULTRA plus electron microscope operating at 3.0 kV. The samples for SEM measurements were dropped and dried on a piece of silicon wafer. Mean particle sizes and standard deviations were obtained by measuring the dimensions of at least 80 particles in the SEM images. XRD data of the pure NPs were collected on a D8-Endeavor diffractometer with a mixed Kα1 and Kα2 Cu (λ = 1.5406 Å) source radiation, operated in a Bragg-Brentano geometry.

Typical MSN synthesis: A three-necks 250 mL round bottom flask containing a 20×40 mm olive stir bar was equipped with a thermometer and a pH probe. CTAB (333 mg, 0.92 mmol 5,7 mM), water (160 mL) and freshly prepared NaOH solution (2.0 M, 1.17 mL, 2.33 mmol, 14.6 mM) were added. The reaction mixture was heated to 80 °C ± 1 °C, with stirring at 700 rpm. After the temperature had stabilized, TEOS (1.67 mL, 7.50 mmol, 46.8 mM) was added at once. After 15 minutes, a condenser was adapted. The reaction mixture was stirred for a total duration of 2 h at 80 °C. After cooling, the MSNs were collected by centrifugation, resuspended in ethanol then centrifuged. The latter operation was repeated twice. Aliquots for SEM were taken at this stage. After drying (60 °C overnight), the surfactant was removed by calcination (2 h at 550 °C, heating rate 10 °C/min).

MSN synthesis with carbonated sodium hydroxide: The above protocol was followed, substituting a volume *V* of the NaOH solution (2.0 M) by 4*V* of $NaHCO_3$ solution (0.5 M).

Results and discussion

The classical MSN synthesis protocol was first evaluated, by adding TEOS (46.8 mM) to a solution of CTAB (5.7 mM), NaOH (14.6 mM) in water at 80 °C with stirring at 700 rpm. The measured starting pH value at 80 °C was 10.5 instead of the 12.1 value that would be expected at 25 °C, which is explained by the high self-ionization constant of water at 80 °C when compared to its value at room temperature (pK_w 12.6 and 13.9 at 75 and 25 °C, respectively).[22] Immediately after the one-shot addition of TEOS (t_0 = 0 s), a fast pH decrease occurs within the first minute, reaching a

minimum at pH 9.3 before slowly raising to reach a final value of 9.5 at the end of the synthesis (Figure 1). This low final value is indeed due to the presence of deprotonated silanols within the nanoparticles, which consumed hydroxide anions from the reaction medium. Overall, these results tend to indicate that the first minute is dominated by the hydrolysis reactions, and that the condensation slowly takes over afterwards. It is noteworthy that the nucleation of NPs also takes place during this first minute, the mixture becoming cloudy after *ca* 45 s. Furthermore, no detectable temperature variation occurs during the first minutes, thus thermal effects can be neglected in this study. Considering the time resolution of the light scattering and pH measurements is close to the second, we decided to investigate in more details the kinetics of the early stages of the process (Figure 1). During the first seconds, a linear decrease of the pH is observed, suggesting that the hydrolysis of TEOS is the only process occurring with a partial first order relative to the hydroxide ions (Phase *Ia*).[16, 23] Then, and unexpectedly, a more pronounced decrease is observed after time t_1 = 17 s (Phase *Ib*), with a sudden change of slope at t_1. At t_2 = 40 s, the pH stops to decrease, and reaches a plateau or even increases slightly for a few seconds (Phase *II*), before starting to decrease again, but with a much lower slope.

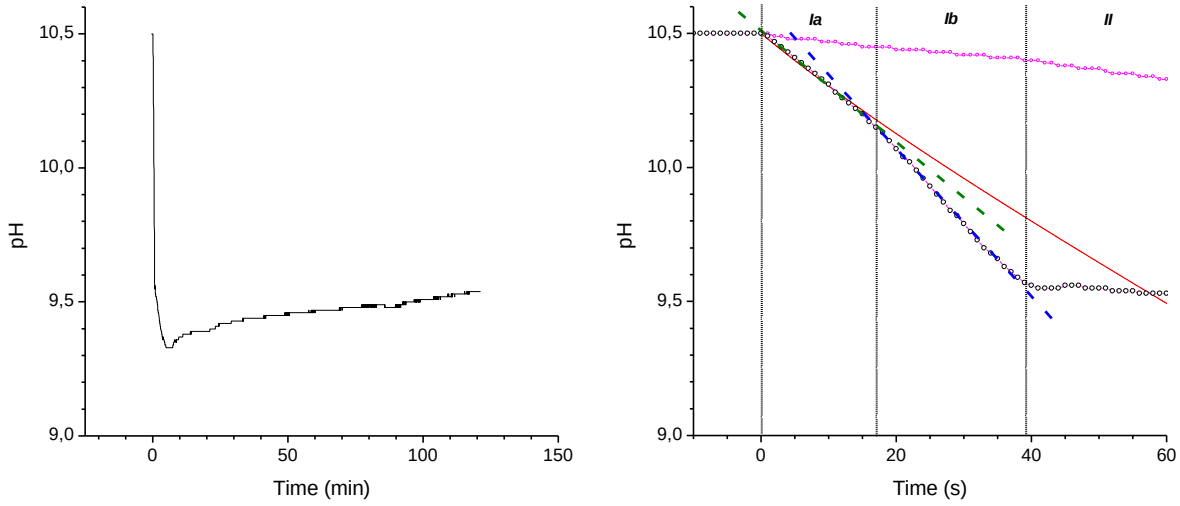

Figure 1: Evolution of the pH during the MSN synthesis: (left) full view over the two hours of synthesis; (right) zoom on the first minute. Reaction performed (black) in the presence and (pink) in the absence of CTAB; The green and blue lines depict two linear regimes of the pH decrease. The red line depicts the calculated pH evolution in the case of a first order reaction for both sodium hydroxide and TEOS.

It is noteworthy that a sharp increase in scattered light intensity occurs at t_2, concomitantly with the plateau of the pH (Figure 2). This scattered intensity then reaches a plateau at the end of Phase II. As the scattered light intensity varies linearly with the concentration of scattering species and their diameter at the power 6, this result suggests that the nanoparticles have reached their final size yet at this stage. The pH variation between t_0 and t_2 enables determining that the $(EtO)_3SiO^-$ concentration is 13 mM, *ie* 28% of the initial TEOS amount at nucleation, under the hypothesis that only singly hydrolyzed species are present at t_2. This synthesis resulted in roughly spherical NPs with a diameter of 89±12 nm, with a 2D hexagonal structure of the pores (Figure 2 and S1c).

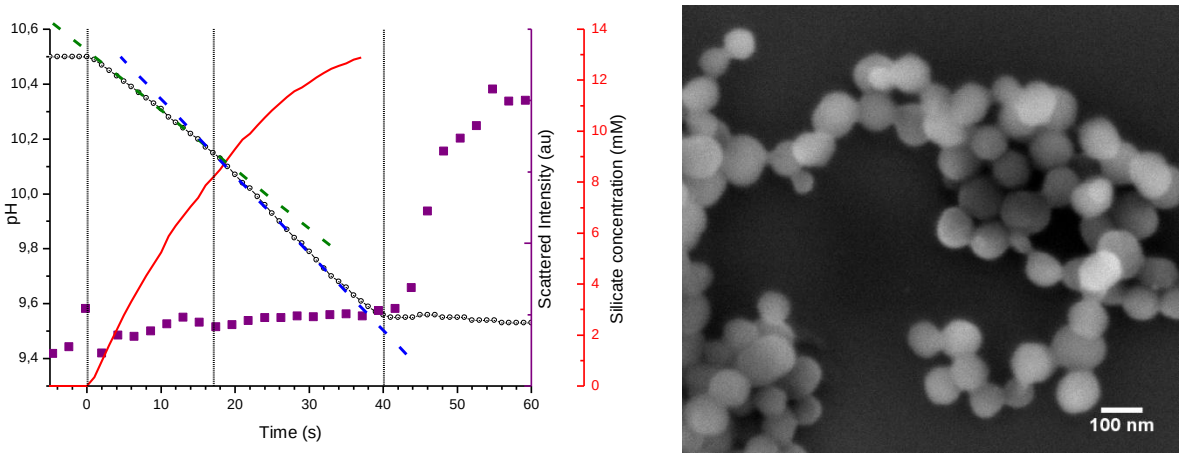

Figure 2: (left) Reaction kinetics monitored by (black dots) pH and (purple squares) light scattering. The red line shows the evolution of the triethoxysilanolate concentration, calculated from the pH decrease. (right) SEM micrograph of the MSNs obtained after synthesis, with a diameter of 89±12 nm.

Notably, the same reaction conducted in the absence of CTAB is characterized by a much slower kinetics, with a factor of *ca* 8 between the initial hydrolysis rates (Figure 1). To better understand the role of the surfactant, experiments were performed by varying its concentration between 2.9 and 7 mM (Figure 3 and S1), *ie* above the first critical micelle concentration determined at 80 °C and 14.8 mM NaOH to be 1.4 mM. A clear increase in rate constant is observed when the CTAB concentration is increased up to 6 mM, with no more increase above this value. Similarly, the stirring speed plays an important role, faster kinetics being observed when the stirring speed is increased. These observations suggest that the hydrolysis reaction mainly takes place at the surface of CTAB micelles, as TEOS is not miscible with water. Such a micellar catalysis was already suggested for the room-temperature hydrolysis and condensation of TEOS at high concentrations of CTAC (0.12 M), with an acceleration factor close to 2000 under such conditions.[24] Accordingly, CTAB is able to encapsulate TEOS within inflated micelles, smaller micelles with higher surface over volume ratio being obtained when the stirring speed is increased, and more micelles being present as the concentration is increased, yielding an overall faster hydroxide consumption. The presence of micelles swollen with TEOS was indeed characterized by SAXS investigations, but for a much higher CTAB concentration.[20] Replacing CTAB by CTAC under identical concentrations led to slower kinetics. CTAC is known to form micelles with lower aggregation number, as a result of weaker coordination of chloride anions with respect to bromide.[25] Using CTAC, larger and more polydisperse NPs were obtained compared with CTAB, while keeping a good pore organization (Figure S2). The strength of stirring (Figure 3), which depends on the stir bar size, stirring speed and shape of the reaction vessel was found to play an important role on the reaction kinetics. Under otherwise constant conditions, we found that the reaction rate increases with the stirring speed between 200 and 400 rpm, being then constant above this value.

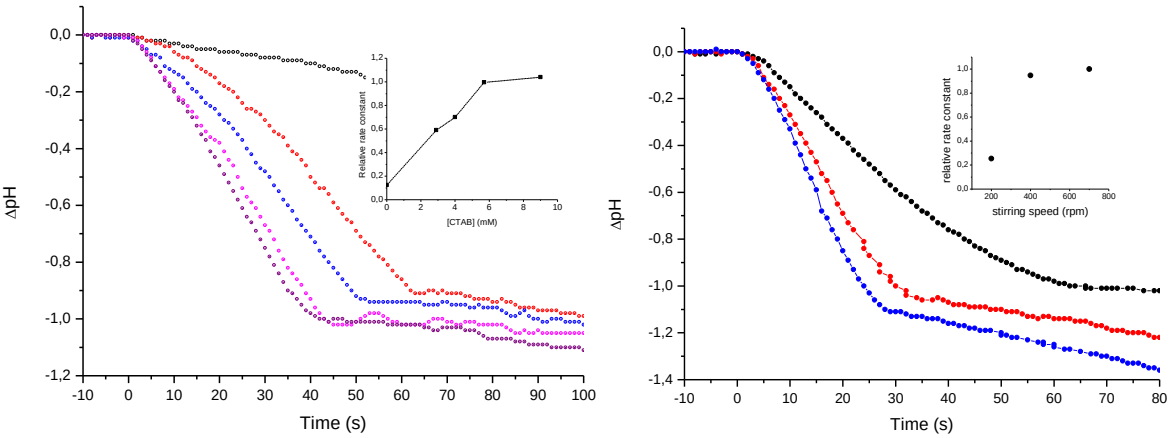

Figure 3: (Left) Dependence of the pH decrease on the CTAB concentration with [CTAB]= (black) 0.0; (red) 2.9; (blue) 4.0; (pink) 5.7; (purple) 7.0 mM. Inset: Evolution of the kinetic constant depending on the CTAB concentration. (Right) Dependence of the pH decrease on the stirring speed with r = (black) 200 rpm; (red) 400 rpm; (blue) 700 rpm. Inset: relative kinetic constant depending on the stirring rate.

An important factor leading to experimental discrepancies is the amount of carbonates in the sodium hydroxide solutions, which is reported to reach up to 40%$_{mol}$.[11] Thus we tested the influence of substituting part of the sodium hydroxide by sodium hydrogen carbonate to simulate the carbonatation of soda (Figure 4 and S3). Unexpectedly, we found that the hydrolysis kinetics were strongly enhanced by the presence of low amounts of sodium carbonate, the rate constant being almost doubled at 10%$_{mol}$ of carbonatation. This increase in rate constant is accompanied by a strong decrease in the size of the final MSNs. Indeed, starting from 90 ± 12 nm for freshly prepared sodium hydroxide, the diameter decreases down to 37±5 nm for sodium hydroxide bearing 40% of $NaHCO_3$. These results corroborate those by Varache *et al* [11] who reported that aggregated small MSNs were obtained for a highly carbonated sodium hydroxide solution. Altogether, these results show that freshly prepared sodium hydroxide solutions must be used for this kind of synthesis.

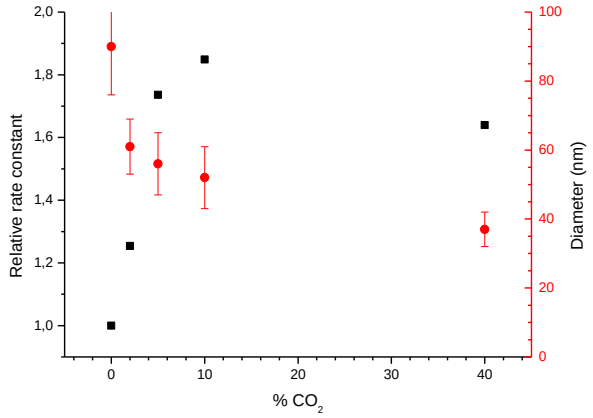

Figure 4: Dependence of the size and rate constant on the carbonatation of sodium hydroxide. (black squares) diameter; (red dots) relative rate constant.

The TEOS concentration was varied in the 10-80 mM range (Figure 5 and S4). A strong effect is observed on the hydrolysis kinetic constant as the TEOS concentration varies, with a linear increase at low to moderate concentrations, which is indeed coherent with first order kinetics with respect to

TEOS [23]. However, the increase of kinetic constant stops for higher concentrations. The nucleation time t_2 is also strongly affected by the TEOS concentration, with no nucleation being observed for the lowest concentration of 10 mM. Indeed, this value is lower than the threshold of *ca* 12-13 mM of silicates at which the aggregates start to form for higher TEOS concentrations. At low TEOS concentration (20 mM), the MSNs feature a large size dispersion and a bad organization of the pores. For higher concentrations (46-80 mM), the diameter is constant (90 ±12 nm) and the MSNs feature a *P6mm* pore organization (Figure S4). Temperature has been reported as a determining factor for the pore organization and size of the MSNs [8]. As expected, the reaction rate increases when the temperature increases over the range 60-90 °C (Figure S5), and the diameter also increases as already reported. However, and by contrast with the published results[8], we found that the organization of the pores within the structure was worse at high temperature, a good pore organization after calcination being observed between 60 and 80 °C (Figure S6).

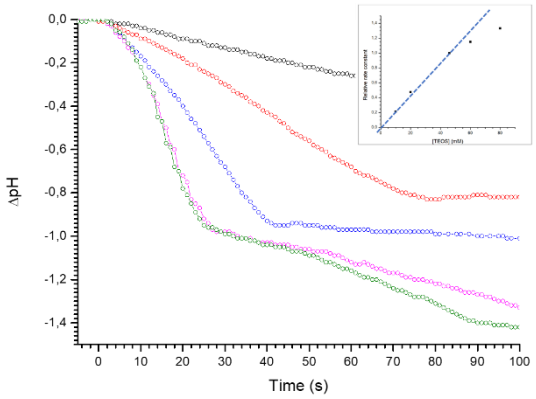

Figure 5: Effect of the TEOS concentration on the reaction kinetics. (black) 10 mM; (red) 20 mM; (blue) 47 mM; (pink) 60 mM; green 80 mM. Inset: dependency of the first relative kinetic constant on the TEOS concentration. The blue line depicts the linear fit on the first data points.

Discussion:

The formation mechanism of MCM-41 materials has been studied by various groups since the first proposals from the seminal 1992 articles [26, 27]. Two kinds of mechanisms were proposed: in the first one, called true liquid crystal templating, a liquid crystal of 2D hexagonal symmetry would be present in solution then hydrolyzed TEOS would hydrolyze and condense in the voids between the rod-like micelles to form the walls of the MCM-41 structure around the micellar template. In the second mechanism, referred to as cooperative self-assembly, the CTAB surfactant would be initially present as spherical micelles and it is only as the TEOS hydrolyzes that the micelles would undergo a transition from spherical to rod-like then to a 2D-hexagonal arrangement. Though numerous reviews and research articles inappropriately mention the true liquid crystal templating as the actual mechanism for MSN synthesis, the CTAB concentrations at which MSNs are prepared (2-20 mM, 0.7-7 g/L) are much closer to the first critical micellar concentration than to the concentration required to achieve liquid crystals in solution (*ca* 40 % wt) or even ellipsoidal micelles (0.1-0.4 M).[24, 28, 29] Even at a high surfactant concentration of 30 g/L, *ie* 80 mM, Yi *et al* showed by SAXS that only ellipsoidal micelles of CTAB swollen with TEOS were present at the beginning of the synthesis [20]. The formation of rod-like micelles was found to occur above 0.2 M at 30 °C, and at higher concentrations when the temperature increases, according to viscosity measurements.[30]

In all above-mentioned mechanistic studies, the focus was placed on the evolution of the micellar component, but much less on the silicate species. Indeed, under typical conditions,[7] most of the

structure is formed within 2-3 minutes which precludes the use of analytical tools such as ^{29}Si NMR in solution. The pH monitoring having a time response of *ca* 1 s, it makes possible to monitor *in situ* the early stages of hydrolysis and condensation by pH changes. Furthermore, *in situ* light scattering measurements allow to precisely determine the turning point at which the nanoparticles start to form. In Figure 2, the first 15 s of the reaction are marked by a linear decrease of the pH, which indicates that the hydrolysis is the only reaction taking place. The much slower hydrolysis of TEOS in the absence of CTAB indicates that TEOS hydrolysis occurs at the interface between the micelle and the aqueous domain, but not at the surface of hypothetical TEOS droplets. However, an efficient mixing is required in order to efficiently encapsulate the TEOS within the micelles, as evidenced by the decrease of the rate constant when the stirring speed is reduced to less than 400 rpm (Figure 3). The first hydrolysis regime (Phase Ia) can be adequately described as pseudo first-order. However, an abrupt transition is observed at t_1 towards a new pseudo first order regime, characterized by a faster pH decrease, which rules out the occurrence of condensation at this stage, which would tend to increase the pH. The hydrolysis of mono-hydrolyzed TEOS to dihydrolyzed TEOS[14] with a rate constant k_2 would only have an influence on the pH if a doubly deprotonated silanediol would be formed, according to equations (4) and (5).

$$\text{=Si(OEt)(O)}^- + \text{OH}^- \rightarrow \text{=}Si(O)_2^{2-} + \text{EtOH} \qquad (4)$$

$$\text{=Si(OEt)(O)}^- + \text{H}_2\text{O} \rightarrow \text{=Si(OH)(O)}^- + \text{EtOH} \qquad (5)$$

However, numerical simulations at various k_2/k_1 ratio (Figure S7) show that in neither case would an abrupt change of slope occur. Therefore, we conclude that t_1 may correspond to a physical change in the shape of the CTAB micelles swollen with TEOS, that leads to more accessible TEOS molecules at their surface, and hence to faster kinetics. We therefore propose that a change from spherical to elongated micelles occurs at t_1, after a concentration of *ca* 9 mM of singly-hydrolyzed TEOS has been reached. When the silicate concentration reaches *ca* 13 mM at t_2, the nucleation of a new phase occurs, which is indicated by the strong raise of the turbidity detected by light scattering measurements (Figure 2). This phenomenon can be attributed to the aggregation of wormlike micelles into micelle bundles.[12] Interestingly, the appearance of the new phase occurs simultaneously with a strong change in pH evolution. Indeed, the pH reaches a plateau around t_2, which means that either the hydrolysis stops or that both hydrolysis and condensation reactions occur at the same rate from this time, which seems more likely. Indeed, as silicate-covered micelles aggregate, the condensation between adjacent silicates in the interstices between micelles becomes favored, with the release of hydroxide anions. These anions are then used in the hydrolysis of unreacted ethoxysilane moieties.

Based on our experimental results and on those published in the literature,[12, 17, 18, 20] the mechanism depicted in Figure 6 can be proposed. TEOS droplets are first dispersed in water thanks to the CTAB surfactant within spherical micelles.[20] TEOS then gets hydrolyzed by the hydroxide ions (Equation (1)) at the interface between the hydrophobic core in the micelles and the aqueous medium, following first order kinetics on both TEOS and OH^- (Phase Ia). The resulting singly-hydrolyzed silanolates adsorb at the micelles surface by strong electrostatic forces. At t_1, a sudden change from spherical to short rod-like micelles occurs, as *ca* 8 mM of TEOS is hydrolyzed. This results in the redistribution of the TEOS molecules within the micelles, with an increase in hydrolysis rate (Phase Ib). At t_2, the micelles aggregate as the hydrolyzed TEOS concentration reaches 13 mM and condensation between neighboring silanes start to occur, at a similar rate (Phase II). Then the pH decreases again slowly, with concomitant fast hydrolysis and condensation reactions. The pH reaches a minimum after 5 minutes, and slowly raises again as the condensation rate becomes faster than the hydrolysis. The pH reaches an asymptotic value of *ca* 9.5 after 2 hours of reaction, which is explained by the presence of deprotonated silanol functions at the surface of the MSNs and of their pores. Unfortunately, it was not possible to measure the amount of ethanol released over time, which would be a good indicator of the progress of the reaction, as ethanol is formed by both hydrolysis and

condensation reactions. Nevertheless, we can assume that the hydrolysis reaction accelerates after t_2, as the micelles are in close contact and hydroxide anions are liberated at the surface of the CTAB micelles swollen with TEOS. The proposed mechanism is in good agreement with the swelling-shrinking model proposed by Yi *et al*.[20] It is also fully compatible with the nucleation model proposed by Sadasivan *et al* [17], though the experimental conditions are substantially different.

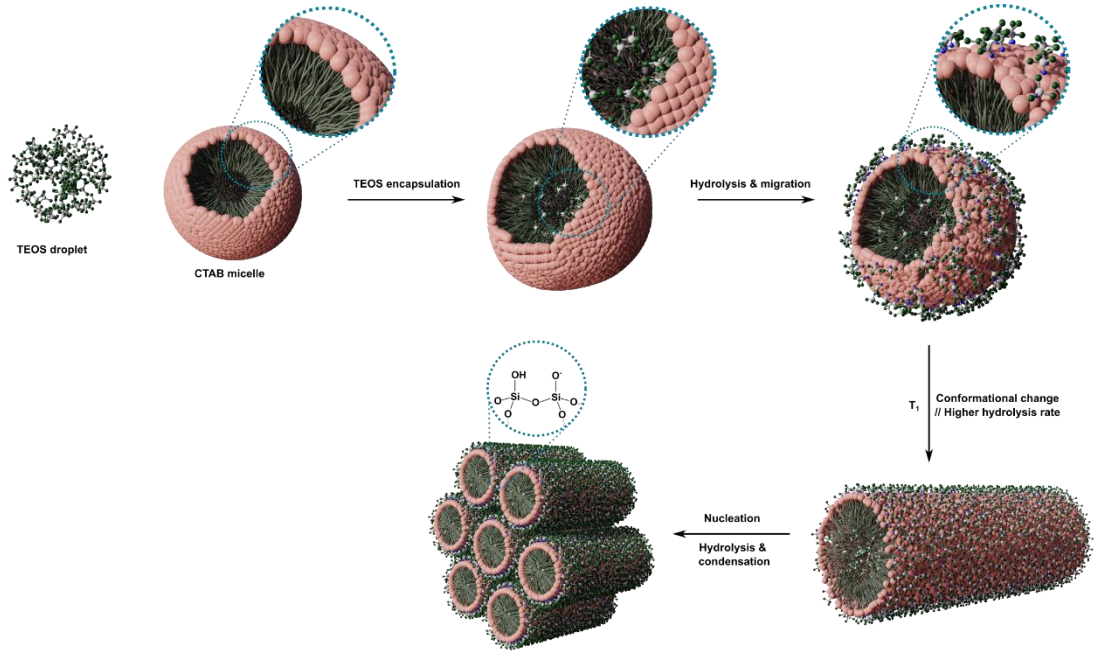

Figure 6: proposed mechanism for the early stages of the synthesis of MSNs.

In conclusion, monitoring the pH during the synthesis of MSNs enables to understand the physico-chemical processes occurring during the early stages of their formation. The hydrolysis mechanism is bimolecular with a first order on both TEOS and OH^- at the early stages, with a strong dependence of the rate constant on the CTAB concentration which is a signature of micellar catalysis. Importantly, we found that sol-gel condensation reactions only start after the nucleation of CTA^+-silicate micelles as hexagonal 2D assemblies of elongated micelles. The nucleation indeed occurs at low TEOS conversion. Though no correlation could be found between the hydrolysis rate and the NPs size or pore organization, some factors strongly affecting the kinetics such as stirring speed and carbonatation of the sodium hydroxide solution may explain the lack of reproducibility of the MSNs synthesis depending on the authors. Much care must therefore be taken to control well all these factors to reproduce or scale up such MSNs synthesis.

References

1. Vallet-Regí M, Schüth F, Lozano D, et al (2022) Engineering mesoporous silica nanoparticles for drug delivery: where are we after two decades? Chem Soc Rev 51:5365–5451. https://doi.org/10.1039/D1CS00659B

2. Kachbouri S, Elaloui E, Charnay C (2022) Synthesis and characterization of a new silica nanoparticles using APG/CTAB as modified agent. J Sol-Gel Sci Technol 103:39–49. https://doi.org/10.1007/s10971-022-05802-3

3. Beltrán-Osuna ÁA, Perilla JE (2016) Colloidal and spherical mesoporous silica particles: synthesis and new technologies for delivery applications. J Sol-Gel Sci Technol 77:480–496.

https://doi.org/10.1007/s10971-015-3874-2

4. Wu S-H, Mou C-Y, Lin H-P (2013) Synthesis of mesoporous silica nanoparticles. Chem Soc Rev 42:3862–3875. https://doi.org/10.1039/C3CS35405A

5. Pal N, Lee J-H, Cho E-B (2020) Recent Trends in Morphology-Controlled Synthesis and Application of Mesoporous Silica Nanoparticles. Nanomaterials 10:2122

6. Florensa M, Llenas M, Medina-Gutiérrez E, et al (2022) Key Parameters for the Rational Design, Synthesis, and Functionalization of Biocompatible Mesoporous Silica Nanoparticles. Pharmaceutics 14:2703

7. Lai C-Y, Trewyn BG, Jeftinija DM, et al (2003) A Mesoporous Silica Nanosphere-Based Carrier System with Chemically Removable CdS Nanoparticle Caps for Stimuli-Responsive Controlled Release of Neurotransmitters and Drug Molecules. J Am Chem Soc 125:4451–4459. https://doi.org/10.1021/ja028650l

8. Catalano F, Pompa PP (2019) Design Rules for Mesoporous Silica toward the Nanosize: A Systematic Study. ACS Appl Mater Interfaces 11:47237–47246. https://doi.org/10.1021/acsami.9b16135

9. Kim M-K, Ki D-H, Na Y-G, et al (2021) Optimization of Mesoporous Silica Nanoparticles through Statistical Design of Experiment and the Application for the Anticancer Drug. Pharmaceutics 13:184. https://doi.org/10.3390/pharmaceutics13020184

10. Castillo RR, de la Torre L, García-Ochoa F, et al (2020) Production of MCM-41 Nanoparticles with Control of Particle Size and Structural Properties: Optimizing Operational Conditions during Scale-Up. Int. J. Mol. Sci. 21:7899

11. Varache M, Bezverkhyy I, Saviot L, et al (2015) Optimization of MCM-41 type silica nanoparticles for biological applications: Control of size and absence of aggregation and cell cytotoxicity. J Non Cryst Solids 408:87–97. https://doi.org/https://doi.org/10.1016/j.jnoncrysol.2014.10.020

12. Ribeiro T, Rodrigues AS, Calderon S, et al (2020) Silica nanocarriers with user-defined precise diameters by controlled template self-assembly. J Colloid Interface Sci 561:609–619. https://doi.org/https://doi.org/10.1016/j.jcis.2019.11.036

13. Varache M, Bezverkhyy I, Bouyer F, et al (2015) Improving structural stability of water-dispersed MCM-41 silica nanoparticles through post-synthesis pH aging process. J Nanoparticle Res 17:356. https://doi.org/10.1007/s11051-015-3147-6

14. McNeil KJ, DiCaprio JA, Walsh DA, Pratt RF (1980) Kinetics and mechanism of hydrolysis of a silicate triester, tris(2-methoxyethoxy)phenylsilane. J Am Chem Soc 102:1859–1865. https://doi.org/10.1021/ja00526a015

15. Qiao Z-A, Zhang L, Guo M, et al (2009) Synthesis of Mesoporous Silica Nanoparticles via Controlled Hydrolysis and Condensation of Silicon Alkoxide. Chem Mater 21:3823–3829. https://doi.org/10.1021/cm901335k

16. Issa AA, Luyt AS (2019) Kinetics of Alkoxysilanes and Organoalkoxysilanes Polymerization: A Review. Polymers (Basel). 11:537

17. Sadasivan S, Fowler CE, Khushalani D, Mann S (2002) Nucleation of MCM-41 Nanoparticles by Internal Reorganization of Disordered and Nematic-Like Silica–Surfactant Clusters. Angew Chemie Int Ed 41:2151–2153. https://doi.org/https://doi.org/10.1002/1521-3773(20020617)41:12<2151::AID-ANIE2151>3.0.CO;2-U

18. Hollamby MJ, Borisova D, Brown P, et al (2012) Growth of Mesoporous Silica Nanoparticles Monitored by Time-Resolved Small-Angle Neutron Scattering. Langmuir 28:4425–4433.

https://doi.org/10.1021/la203097x

19. Cabrera S, El Haskouri J, Guillem C, et al (2000) Generalised syntheses of ordered mesoporous oxides: the atrane route. Solid State Sci 2:405–420. https://doi.org/https://doi.org/10.1016/S1293-2558(00)00152-7

20. Yi Z, Dumée LF, Garvey CJ, et al (2015) A New Insight into Growth Mechanism and Kinetics of Mesoporous Silica Nanoparticles by in Situ Small Angle X-ray Scattering. Langmuir 31:8478–8487. https://doi.org/10.1021/acs.langmuir.5b01637

21. Blin JL, Impéror-Clerc M (2013) Mechanism of self-assembly in the synthesis of silica mesoporous materials: in situ studies by X-ray and neutron scattering. Chem Soc Rev 42:4071–4082. https://doi.org/10.1039/C2CS35362H

22. Bandura A V, Lvov SN (2005) The Ionization Constant of Water over Wide Ranges of Temperature and Density. J Phys Chem Ref Data 35:15–30. https://doi.org/10.1063/1.1928231

23. Osterholtz FD, Pohl ER (1992) Kinetics of the hydrolysis and condensation of organofunctional alkoxysilanes: a review. J Adhes Sci Technol 6:127–149. https://doi.org/10.1163/156856192X00106

24. Cheng C-F, Luan Z, Klinowski J (1995) The Role of Surfactant Micelles in the Synthesis of the Mesoporous Molecular Sieve MCM-41. Langmuir 11:2815–2819. https://doi.org/10.1021/la00007a075

25. Zana R, Frasch J, Soulard M, et al (1999) Fluorescence Probing Investigations of the Mechanism of Formation of Organized Mesoporous Silica. Langmuir 15:2603–2606. https://doi.org/10.1021/la981603f

26. Beck JS, Vartuli JC, Roth WJ, et al (1992) A New Family of Mesoporous Molecular Sieves Prepared with Liquid Crystal Templates. J Am Chem Soc 114:10834–10843. https://doi.org/10.1021/ja00053a020

27. Kresge CT, Leonowicz ME, Roth WJ, et al (1992) Ordered mesoporous molecular sieves synthesized by a liquid-crystal template mechanism. Nature 359:710–712. https://doi.org/10.1038/359710a0

28. Raman NK, Anderson MT, Brinker CJ (1996) Template-Based Approaches to the Preparation of Amorphous, Nanoporous Silicas. Chem Mater 8:1682–1701. https://doi.org/10.1021/cm960138+

29. Goyal PS, Dasannacharya BA, Kelkar VK, et al (1991) Shapes and sizes of micelles in CTAB solutions. Phys B Condens Matter 174:196–199. https://doi.org/https://doi.org/10.1016/0921-4526(91)90606-F

30. Kuperkar K, Abezgauz L, Prasad K, Bahadur P (2010) Formation and Growth of Micelles in Dilute Aqueous CTAB Solutions in the Presence of NaNO3 and NaClO3. J Surfactants Deterg 13:293–303. https://doi.org/https://doi.org/10.1007/s11743-009-1173-z

DECLARATION:

Funding: This work was supported by the Agence Nationale de la Recherche (ANR-20-CE09-0017-03).

Competing Interests: *The authors have no relevant financial or non-financial interests to disclose.*

Author Contributions: *All authors contributed to the study conception and design. Material preparation, data collection and analysis were performed by Ricardo Alvarado Meza, Tom Santori and Xavier Cattoën. The first draft of the manuscript was written by Xavier Cattoën and all authors*

commented on previous versions of the manuscript. All authors read and approved the final manuscript.